CASCARANO, G., GIACOVAZZO, C. & GUAGLIARDI, A. (1992). *Acta Cryst.* A**48**, 859–865.
CASCARANO, G., GIACOVAZZO, C. & VITERBO, D. (1987). *Acta Cryst.* A**43**, 22–29.
COCHRAN, W. (1955). *Acta Cryst.* **8**, 473–478.
COCHRAN, W. & DOUGLAS, A. S. (1957). *Proc. R. Soc. London Ser. A*, **243**, 281.
DECLERCQ, J.-P., GERMAIN, G. & WOOLFSON, M. M. (1979). *Acta Cryst.* A**35**, 622–626.
DETITTA, G. T., EDMONDS, J. W., LANGS, D. A. & HAUPTMAN, H. (1975). *Acta Cryst.* A**31**, 472–479.
FERCHAUX, Y., VILLAIN, F. & NAVAZA, A. H. (1990). *Acta Cryst.* C**46**, 346–348.
GIACOVAZZO, C. (1976*a*). *Acta Cryst.* A**32**, 91–99, 100–104.
GIACOVAZZO, C. (1976*b*). *Acta Cryst.* A**32**, 958–966.
GIACOVAZZO, C. (1980). In *Direct Methods in Crystallography*. London: Academic Press.
GIACOVAZZO, C. (1983). *Acta Cryst.* A**39**, 585–592.
GILLIS, J. (1948). *Acta Cryst.* **1**, 76–80.
HARKER, D. & KASPER, J. S. (1948). *Acta Cryst.* **1**, 70–75.
HAUPTMAN, H. (1975). *Acta Cryst.* A**31**, 671–679, 680–687.
HAUPTMAN, H. (1976). *Acta Cryst.* A**32**, 877–882.
HAUPTMAN, H. (1982). *Acta Cryst.* A**38**, 632–641.
KARLE, J. & HAUPTMAN, H. (1950). *Acta Cryst.* **3**, 181–187.
KARLE, J. & HAUPTMAN, H. (1956). *Acta Cryst.* **9**, 635–651.
KARLE, J. & KARLE, I. (1966). *Acta Cryst.* **21**, 849–859.
MACGILLAVRY, C. H. (1950). *Acta Cryst.* **3**, 214–217.
NAVAZA, A. & NAVAZA, J. (1992). *Acta Cryst.* A**48**, 695–700.
OKAYA, J. & NITTA, I. (1952). *Acta Cryst.* **5**, 564–570.
SAYRE, D. (1952). *Acta Cryst.* **5**, 60–65.

Acta Cryst. (1994). A**50**, 317–325

(4;2)-Connected Three-Dimensional Nets Related to the Mixed-Coordinated Framework Structures $AlPO_4$-15, $AlPO_4$-CJ2 and $AlPO_4$-12

BY K. J. ANDRIES AND J. V. SMITH

The Consortium for Theoretical Frameworks, Department of the Geophysical Sciences, The University of Chicago, 5734 South Ellis Avenue, Chicago, Illinois 60637, *USA*

(*Received* 26 *March* 1993; *accepted* 27 *September* 1993)

Abstract

Application of the same pattern for linking neighbouring 4.8^2 two-dimensional nets as is found in the $AlPO_4$-CJ2 and $AlPO_4$-15 structures allows the enumeration of eleven (4;2)-connected three-dimensional nets with a maximum unit-cell repeat of ~ 10 Å. Net 551 is polytypic with net 398 (the tetrahedral analogue of $AlPO_4$-12). The (4;2)-connected nets related to $AlPO_4$-15 (net 400) and $AlPO_4$-CJ2 (net 725) have the highest symmetry of the present nets. Synthetic zeolite Linde J may have the latter framework topology. Nets 400 and 725 relax considerably upon lowering of the space group symmetry. Geometrical refinements indicate that the mixed-coordinated $AlPO_4$-15 is more feasible than its (4;2)-connected relative (same space group symmetry); the feasible net 398 and the topologically simpler net 551 have not been observed so far. Geometrically optimized atomic coordinates are given for the most feasible nets obtained here.

Introduction

Tetrahedrally coordinated frameworks occur in zeolitic materials used in ion exchange, catalysis and molecular sieving. Research is expanding into a wider range of scientific areas as new materials are synthesized [particularly ultra-pore materials, *e.g.* Kresge, Leonowicz, Roth, Vartuli & Beck (1992)]. The *Atlas of Zeolite Structure Types* (Meier & Olson, 1992) and Smith (1988) give references and structural information on most topologically distinct zeolite materials and their three-letter structure-type codes.

The systematic enumeration of (4;2)-connected three-dimensional (3D) nets is important for the characterization and classification of known framework structures as well as for the solution of as yet unknown phases. The notation describes four-connected nodes (*e.g.* silicon, aluminium, phosphorus) bridged by two-connected atoms (*e.g.* oxygen). Omission of the two-connected atoms leaves a fully four-connected net. Some exploratory contributions in the field of theoretical enumeration have come from Wells (1977), Smith (1977, 1978), Alberti (1979), Smith & Bennett (1984), Smith & Dytrych (1986), Hawthorne & Smith (1988), Kokotailo, Fyfe, Gies & Cox (1989), Andries (1990) and O'Keeffe (1992). It is expected that, with the aid of modern computational techniques, more general approaches can be undertaken towards the systematic enumeration of four-connected 3D nets. Four techniques for generating 3D net topologies are: (i) simulated annealing (Deem & Newsam, 1989); (ii) a combinatorial method (Treacy, Rao & Rivin, 1992); (iii) application of stacking operators to two-dimensional

©1994 International Union of Crystallography
Printed in Great Britain – all rights reserved

(2D) sheet structures (Akporiaye & Price, 1989); and (iv) model building. Structural relationships within some restricted groups of zeolitic materials (Akporiaye, 1989, 1992; van Koningsveld, 1992) may provide interesting hints in relation to their nucleation mechanism (Brunner, 1992). A general theory for the systematic enumeration of two-dimensional three-connected nets (Wood & Price, 1992) takes advantage of modern computational techniques that may also facilitate the calculation of complex geometrical properties such as ring statistics (Marians & Hobbs, 1990; Stixrude & Bukowinski, 1990; Goetzke & Klein, 1991).

The enumeration of tetrahedrally coordinated 3D nets belonging to a particular structural group in which some members have already been observed may prove useful as a more profound study of what types of frameworks are most likely to be observed. For the investigation of the geometrical feasibility of 3D nets, two approaches are possible: (i) distance-least-squares (DLS) refinement (Baerlocher, Hepp & Meier, 1977), which optimizes cell parameters and/or atomic coordinates under assumed space-group symmetry, using prescribed values for local geometry parameters (first- and second-neighbour distances and angles that prove rather constant for this type of structure); (ii) calculation of the structural stability by quantum-mechanical *ab initio* or semi-empirical techniques or by minimization of the lattice energy during structure relaxation.

Here, we use the DLS method in the study of tetrahedral nets related to $AlPO_4$-CJ2 (Yu, Pang & Li, 1990), $AlPO_4$-15 (Parise, 1984*b*; Pluth, Smith, Bennett & Cohen, 1984) and $AlPO_4$-12 (Parise, 1984*a*). None of these three materials is fully four-connected (besides four-coordinated phosphorus, they contain five- and/or six-coordinated aluminium) but they can easily be related to such a net. In addition, we investigate to what extent the DLS method might explain the occurrence of some materials as strictly (4;2)-connected while others deviate from this topochemically simplest pattern.

Topologically, both the 3D nets present in $AlPO_4$-CJ2 and $AlPO_4$-15 are based on the same three-connected 2D net (4.8^2, code 'fee', see below) as well as the same pattern according to which neighbouring 'fee' nets are connected (see below). We derive the topologically distinct tetrahedral 3D nets that are obtained under these conditions, further imposing limits on the unit-cell dimensions.

Enumeration

Fig. 1(*a*) represents the 4.8^2 three-connected 2D net (one-sided plane group: *p4mm*; denoted 'fee') occurring in 31 topologically distinct framework structures. Four-connected 3D nets are generated by stacking parallel 2D nets and connecting vertices by assigning an up (*U*)- or down (*D*)-directed fourth branch. We restrict the enumeration to those *U/D* patterns that result in either of the two smallest rectangular 2D unit repeats (Fig. 1*a*, dashed lines). The smallest unit repeat is $\sim 7.2 \times 7.2$ Å (assuming an internodal bond distance of 3.2 Å); the other is $\sim 10.2 \times 10.2$ Å [$7.2(2^{1/2})$]. These dimensions do not necessarily refer to the crystallographic unit repeats for specific *U/D* patterns (see below). The smallest unit repeat does not allow strict alternation of two chemically different atoms in vertex positions; the larger cell does.

The pattern according to which neighbouring 'fee' nets are connected in the structures of $AlPO_4$-CJ2 and $AlPO_4$-15 is given in projection in Fig. 1(*b*). Parallel 2D nets (neighbouring nets are displaced parallel to each other) are indicated in bold full and dashed lines and thin lines represent the intersheet linkages between nodes of adjacent 2D nets (the direction of the intersheet bonds depends on the particular *U/D* pattern of the 4.8^2 net). The third unit-cell dimension is now fixed by assuming that alternating 2D nets are identical and project onto each other in Fig. 1(*b*). We first derive all the *U/D* patterns that are allowed in the 'fee' net under the unit-cell restrictions set forth above; subsequently, we derive the 3D nets obtained by connecting 'fee' nets with the same *U/D* configuration, applying the inter-sheet linking pattern represented in Fig. 1(*b*).

Results

Since no known framework structure is built up (entirely) from the 4.8^2 2D net with different *U/D* sequences in its four-rings (considering inverted sequences to be identical, *e.g. UUUD* and *UDDD*), we further assume that all four-membered rings have the same *U/D* sequence (*UUUU*, *UUUD*, *UUDD* or *UDUD*). Fig. 2 shows the 12 distinct patterns that can be used to generate 3D nets. Vertices marked

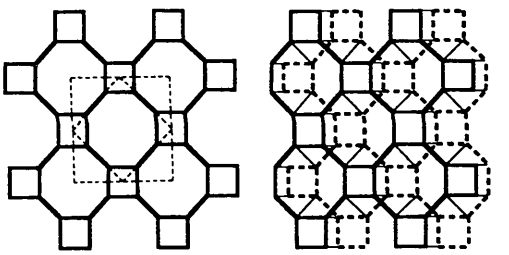

(*a*) (*b*)

Fig. 1. (*a*) The three-connected 4.8^2 ('fee') 2D net. (*b*) Schematic representation of the inter-sheet linking pattern used for the enumeration of 3D nets. Parallel 2D nets: bold full and dashed lines. Intersheet linkages (no distinction between oppositely oriented bonds): thin lines.

with a circle are oppositely oriented to unmarked ones. The first three patterns are the only possible choices with the smallest rectangular unit repeat. Table 1 gives geometric and crystallographic data for the patterns in Fig. 2. The third column in the table gives the node sequence in the eight-rings, as originally introduced by Smith & Rinaldi (1962) (*S* and *C* designate nodes with the same and opposite orientation, respectively, compared with the previous one in the cycle). Two-sided plane groups are given in column 4. Small letters distinguish the 2D lattice type from the 3D Bravais lattice type. For the unit-cell axes, the same conventions are used as in *International Tables for Crystallography* (1983). The axis perpendicular to the 2D net is labelled *c*; *a* and *b* are chosen arbitrarily, except for oblique unit cells where *b* is chosen as the unique axis. The fifth column in Table 1 gives the ratio of oppositely oriented nodes ($N_{UD} \geq 1$).

Table 1. *Geometric and crystallographic data for the 2D patterns in Fig. 2*

N_{2D}	Four-rings	Sequence in eight-rings	Two-sided plane group*	N_{UD}
1	*UUDD*	*SCCCSCCC*	*c*12/*m*1 (12)	1
2	*UDUD*	*SCSCSCSC*	*p*$\bar{4}$*m*2 (115)	1
3	*UUUD*	*SSSCCSCC*	*p*1*m*1 (6)	3
4	*UUUU DDDD*	*SCSCSCSC*	*p*4/*nmm* (129)	1
5	*UUDD*	*SSSCSSSC*	*pman* (53)	1
6	*UUDD*	*SSSCSSSC SCCCSCCC*	*c*12/*m*1 (12)	1
7	*UDUD*	*CCCCCCCC*	*p*4/*nbm* (125)	1
8	*UUUD*	*SSSSSCSC*	*cmm*2 (35)	3
9	*UUUD*	*SSSSCCCC*	*p*1*a*1 (7)	3
10	*UUUD UDDD*	*SSCCCSSC*	*cm*2*a* (39)	1
11	*UUUD UDDD*	*SCCSCSSC*	*p*12$_1$1 (4)	1
12	*UUUD UDDD*	*SCCCCCSC*	*c*12/*m*1 (12)	1

* Numbers in parentheses are topologically highest 3D space group numbers if no higher symmetry were present.

To enumerate 3D nets, copies of the patterns in Fig. 2 were superimposed and all possible displacements and rotations applied. The 11 3D nets thus obtained are schematically represented in projection in Fig. 3. Bold and thin lines are used for parallel 'fee' nets; inter-sheet linkages (dashed and full lines represent oppositely oriented bonds) are also represented by thin lines. Open and filled circles represent nodes with the same orientation in adjacent 2D nets.

Geometric and crystallographic data for these 3D nets (and net 398, see below) are given in Table 2. Entries are: (i) N_{3D} (catalogue number); (ii) the topologically highest space group (and number); (iii) N_{2D} (sequence number in Table 1 of the 2D pattern from which the net is obtained); (iv) Z_c (number of tetrahedral nodes in the crystallographic unit cell); (v)–(x) unit-cell parameters (obtained after DLS refinement, using the highest topological symmetry and an overall *T*–O distance of 1.68 Å; weights associated with *T*–O, O–O and *T*–*T* distances were set at 2.0, 1.0 and 0.2, respectively; occasionally damping factors < 1.0 for atom and/or cell parameter shifts were used); (xi) circuit symbols (Wells, 1977); (xii) R_{DLS}, the DLS geometrical agreement factor; (xiii) the topologically highest space group (and number) for strict *T*-atom alternation. Throughout, the monoclinic and orthorhombic space group settings used are those for $b > a > c$.

The most important polyhedral units, one-dimensional (1D) units (chains, columns and tubes) and 2D planar nets (except the original 'fee' net used to generate the 3D nets) are listed in Table 3. Polyhedral units that are not part of 1D units in the third column of the table are shown in Fig. 4. One-dimensional units are represented in Fig. 5 and 2D planar nets in Fig. 6. The label identifying each structural unit is a mnemonic code from the lists at the Consortium for Theoretical Frameworks of structural units occurring in 3D nets of zeolites and related framework structures. Table 3 does not list polyhedral or 1D units that are part of others in the same 3D net (*e.g.* 'kah' is part of 'kre' in nets 391

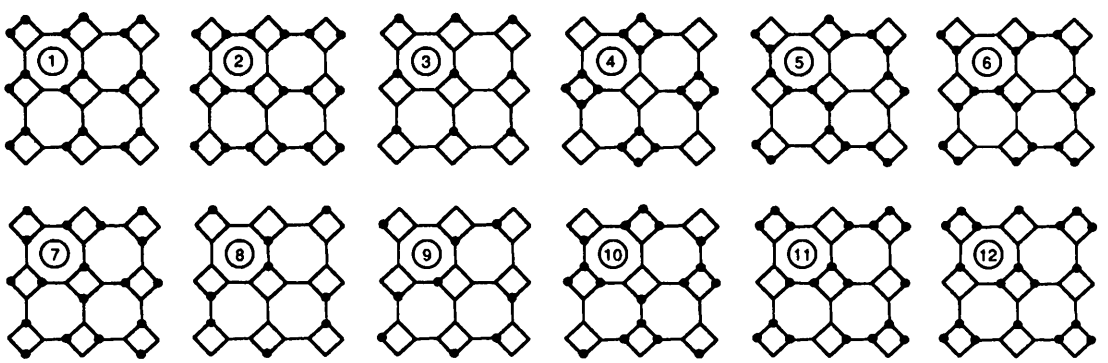

Fig. 2. The 12 two-sided planar patterns with an up or down direction assigned to each vertex (marked and unmarked ones are oppositely oriented), restricted to the two smallest rectangular 2D unit cells in the 'fee' net. Numbers are sequence numbers in Table 1.

Table 2. *Geometric and crystallographic data for the 3D nets in Fig. 3 and net 398*

N_{3D}	Highest space group	N_{2D}	Z_c	a (Å)	b (Å)	c (Å)	α (°)	β (°)	γ (°)	Circuit symbols	R_{DLS}	Space group for alternation
389	$P112_1/b$ (14)	10	16	10.51	14.50	9.04	–	–	136.65	$(4^36^28^1)_1(4^26^38^1)_1$ $(4^26^28^2)_1(4^16^48^1)_1$	0.0067	$P112_1$ (4)
390	$Pnn2$ (34)	10	16	8.76	11.05	7.14	–	–	–	$(4^46^2)_1(4^26^28^2)_1$ $(4^26^28^2)_1(4^26^18^3)_1$	0.0151	$P1a1$ (7)
391	$C211$ (5)	3	16	9.82	10.47	9.43	89.92	–	–	$(4^36^28^1)_1(4^26^28^2)_1$ $(4^26^28^2)_1(4^16^28^3)_1$	0.0051	$P2_111$ (4)
392	$P\bar{1}$ (2)	3	8	7.29	9.04	7.25	82.18	90.75	115.51	$(4^36^28^1)_1(4^36^28^1)_1$ $(4^36^18^2)_1(4^16^18^4)_1$	0.0066	$P\bar{1}$ (2)
393	$P2/b11$ (13)	9	16	8.73	10.77	7.18	86.79	–	–	$(4^46^2)_1(4^36^28^1)_1$ $(4^26^38^1)_1(4^16^38^110^1)_1$	0.0159	$Pb11$ (7)
394	$P2/b11$ (13)	9	16	9.78	10.75	8.71	86.35	–	–	$(4^36^3)_1(4^36^28^1)_1$ $(4^16^48^1)_1(4^16^410^1)_1$	0.0069	$Pb11$ (7)
398*	$B112/m$ (12)	1	24	10.29	14.04	9.70	–	–	98.65	$(4^26^4)_1(4^26^38^1)_1$ $(4^16^48^1)_1$	0.0058	$P112_1/a$ (14)
400	$Cmca$ (64)	11	32	10.96	15.34	9.80	–	..	–	$(4^36^28^1)_1(4^38^3)_1$ $(4^26^18^3)_1(4^28^4)_1$	0.0084	$Cmca$ (64)
551	$C2/m11$ (12)	1	16	9.73	10.11	8.96	90.72	–	–	$(4^26^4)_1(4^16^48^1)_1$	0.0034	$P2_1/b11$ (14)
725	$P4_12_12$ (92)	11	16	9.32	9.32	10.88	–	–	–	$(4^26^28^2)_1(4^26^28^2)_1$	0.0044	$P2_12_12_1$ (19)
958	$Pnnb$ (52)	7	16	8.69	10.88	7.87	–	–	–	$(4^16^5)_1(4^16^48^1)_1$	0.0168	$P2_1nb$ (33)
959	$Pbnn$ (52)	5	16	8.54	11.29	6.63†	–	–	–	$(4^36^28^1)_1(4^36^28^1)_1$	0.0097	$Pbn2_1$ (33)

* Net 398 (the tetrahedral equivalent of $AlPO_4$-12) is polytypic with net 551.

† DLS refinement of net 959 without supplementary restrictions results in nonbonded intersheet T–T distances that are smaller than bonded ones. The nonbonded interplanar T–T distance was therefore constrained at 3.5 Å.

and 394 and 'fhe' is part of 'kek' in net 725). Underlined codes in column 4 of Table 3 denote 2D nets that stack onto each other to build up the entire 3D net. The number in superscript in the same column is the number of crystallographic directions in which the 2D net occurs. Column 5 in Table 3 indicates the occurrence of straight channels in some nets (*nR*: *n*-membered channel entrance ring; *nD*: dimensionality of the channel system). Table 4 is a compilation of geometric and crystallographic data for the structural units listed in Table 3. The face symbol lists all polygons bounding the polyhedral unit with the number in each symmetrically equivalent set in superscript. In the 1D rod group notation, a three (or higher)-fold symmetry chain axis is given first; in all other cases, the third axis symbol refers to the chain axis. *R* is the minimum number of connecting edges in the chain repeat and along the chain

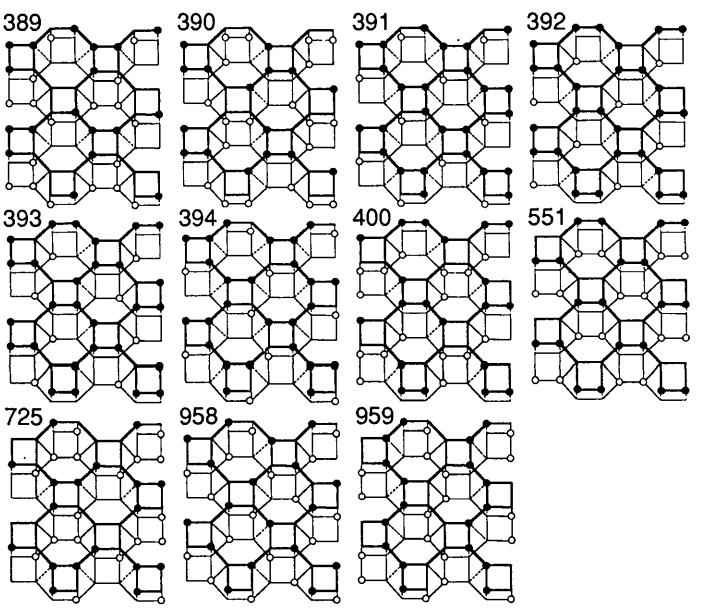

Fig. 3. The 11 3D nets. Numbers are catalogue numbers (Table 2). Parallel 'fee' nets: bold and thin lines. Intersheet linkages (oppositely oriented bonds: dashed and full lines): thin lines. Open and filled circles represent equally oriented nodes in adjacent 2D nets.

Table 3. *Structural units (SU) and channels in the 3D nets*

N_{3D}	SU_{3D}	SU_{1D}	SU_{2D}*	Straight channels
400	krz, kjr	*z*, fhe, kys, kyt	fee, vvv	
551	vvs, lau, kzb	apt, thr, ken, keu, kew, kyy, kyz, kza	hex, fsy, fos	
725	krb	kek, krc	fee, fto^4	
958	kah	*z*, kbg	hex, hex^2	
959		*z*, *c*		8*R* (1D)
389	krb	krc, krd	fsv, hex, ffs, fto^2	
390	iet, kyx	*z*	fsv, ffs^2, vvv^2	
391	kre	kbg, krc	fsv, brw^2	8*R* (2D)†
392	krl, kds	*z*, krh, krk, krm, krn	fsv, brw, vvv	8*R* (2D)†
393	krt	*z*, kru	hex, fvo^2	10*R* (1D)‡
394	kre, kre§	kbg, krd	hex, ftn^2	10*R* (1D)‡

* Underlined codes are 2D nets that stack onto each other to build up the 3D net; the number of crystallographic directions in which the 2D net occurs is given by superscripts.

† Channel system intersecting through eight-ring windows.

‡ Highly elliptical ten-rings.

§ Enantiomorphic configuration.

axis, *N* gives the number of nodes in the chain repeat and *d* represents the approximate chain-repeat distance (in Å). In the circuit symbols for 2D nets, the relative numbers of symmetrically non-equivalent nodes are given as subscripts.

Discussion

Net 389 is built from 1D units that are also found in other nets of this series ('krc' and 'krd'). The topological symmetry is rather low and reducing the space group symmetry to that for alternation reduces the R_{DLS} factor only slightly (0.0063). DLS refinements in the space group for alternation were done using Si–O and Al–O bond distances of 1.63 and 1.74 Å, respectively, and the same weighting scheme as given above.

Nets 390, 393 and 958 are not geometrically feasible (Table 2, $R_{DLS} > 0.015$). Lowering the space group symmetry to that for alternation (or lower)

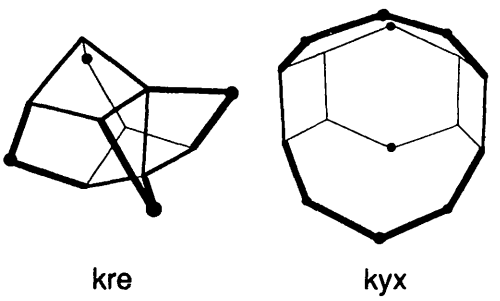

Fig. 4. Polyhedral units not occurring in 1D chains listed in column 3 of Table 3. Two-connected vertices are represented by dots whose size shows view depth.

Table 4. *Geometric and crystallographic data for polyhedral units, 1D units and 2D nets in Table 3*

Code	Crystallographic group	Description
Polyhedral units	Point group	Face symbol
kzc	*m*	$4^1 4^1 6^2 6^1 8^1 8^1$
krt	2	$4^2 4^2 4^2 4^2 6^2 8^2$
krl	$\bar{1}$	$4^2 4^2 4^2 4^2 6^2 8^2$
kre	2	$4^2 4^2 6^2 6^1$
kzb	2/*m*	$4^2 4^2 6^2 6^2 6^2 8^2$
vvs	2/*m*	$4^2 4^2 6^4 8^2$
kyx	*mm*2	$4^2 6^1 8^2 10^1$
krb	2	$4^2 6^2$
kdq	*mm*2	$4^2 6^2 8^2$
lau	4/*mmm*	$4^2 6^4$
kds	*mmm*	$4^2 8^2$
kjr	*mmm*	$4^2 8^4$
iet	3*m*	$4^3 6^1$
krz	2/*m*	$4^4 4^2 8^4$
kaa	*mmm*	$6^2 8^2$
kah	$\bar{6}2m$	6^3
Two-dimensional nets	Plane group	Circuit symbols
hex	*p*6*mm*	6^3
ffs	*c*2*mm*	$(4^2 10)_1 (4.10^2)_2$
fos	*c*2*mm*	$(4^2 12)_1 (4.12^2)_1$
fsy	*c*2*mm*	$(4.6.8)_1 (6^2 8)_1$
brw	*p*2*mm*	$(4.6.8)_2 (6.8^2)_1$
fsv	*p*2*mm*	$(4^2 10)_1 (4.6.10)_2 (6.10^2)_1$
vvv	*p*2*mm*	$(4^2 12)_1 (4.8.12)_1 (4.8.12)_1$
fto	*p*2*mg*	$(4.6.8)_1 (4.8^2)_1 (6^2 8)_1$
ftn	*p*2*mm*	$(4^2 10)_1 (4.6.10)_2 (6^3)_1 (6^2.10)_2$
fvo	*p*2*mm*	$(4^2 14)_2 (4^2 14)_1 (4.6.14)_2 (6.14^2)_1$
One-dimensional units	Rod group	*R*, *N*, *d*
z	*pcmm*	2, 2, 5
krn	*p*2/*m*11	3, 8, 7
krh	$p\bar{1}$	3, 8, 7
apt	*p*2/*m*11	3, 10, 7
kyy	$p\bar{1}$	3, 10, 7
krk	*pmmm*	3, 14, 7.5
fhe	$p4_122$	4, 4, 9
c	*pcmm*	4, 4, 8.5
kbg	$p\bar{6}2m$	4, 8, 8.5
kek	$p4_122$	4, 12, 10
thr	*pmmm*	4, 12, 8.5
kyz	*p*2/*m*11	4, 12, 8.5
krc	$p112_1$	4, 12, 8.5
krd	$p\bar{1}$	4, 12, 8.5
ken	*pcmm*	4, 16, 8.5
kys	*p*2/*m*11	4, 16, 10
keu	*p*2/*m*11	4, 16, 9.5
kew	*p*2/*m*11	4, 16, 10
kru	*p*211	4, 16, 10.5
krm	$p\bar{1}$	4, 16, 10
kyt	$p\bar{1}$	4, 16, 10
kza	*p*2/*m*11	8, 32, 20

does not reduce the R_{DLS} factor significantly. The unfeasibility of nets 390 and 393 may be attributed to the presence of a structural unit that is built from 'iet' polyhedral units [this is the secondary building unit (Meier & Olson, 1992) with face symbol 4^36^1 and point group symmetry $3m$] that in pairs share a common four-ring and are symmetry-related by a twofold rotation axis. In net 393, these polyhedral units are part of 'kru' 1D units that build dense 2D layers by sharing common four- and six-rings.

Net 391 contains the 'krc' 1D unit, also found in nets 725 and 389. It is built from dense 2D layers, made up of edge-sharing 'kre' polyhedral units. In the space group for alternation, the R_{DLS} factor is 0.0048.

Net 392 contains 'double open cubes' (see below; also found in net 400) that share edges in chain 'krh'. This chain contains a ladder-like 1D unit and is related to the 'odc' chain (Smith, 1988) found in the mixed-coordinated $GaPO_4$-14 framework (Parise, 1985*a*) but has a smaller chain repeat. Net 392 is built from dense 2D layers, made up of 'krm' chains that share common four- and six-rings. The R_{DLS} factor in the space group for alternation is 0.0061.

Net 394 contains a ladder-like 1D unit and is related to net 391, being built from similar dense 2D layers. In net 394, these layers are built up with both the left and right enantiomers of the 'kre' polyhedral unit (edge sharing). The R_{DLS} factor in the space group for alternation is 0.0063. Net 394 is the only geometrically feasible net obtained in this study with channels having an entrance ring larger than an $8T$-atom ring.

Net 400 is the (4;2)-connected analogue of $AlPO_4$-15 (Parise, 1984*b*; Pluth, Smith, Bennett & Cohen, 1984). It is built entirely from 'kys' and 'kyt' 1D units. A polyhedral unit worth mentioning is the 'double open cube' (not coded; built from two 'iet' polyhedral units that in pairs share a common four-ring and are symmetry related by an inversion centre), which is part of the 'kys' chain and occurs also in net 392. In net 400, these units share vertices. A description of $AlPO_4$-15 and related net 400 is provided by Bennett, Dytrych, Pluth, Richardson &

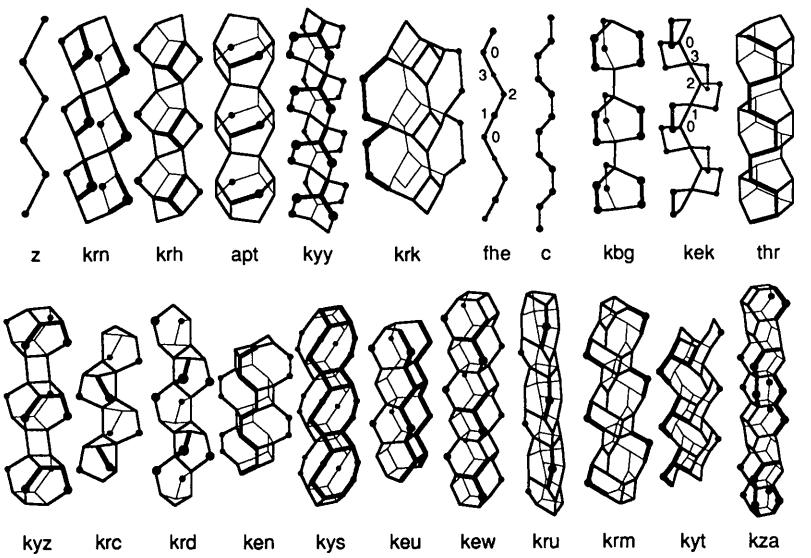

Fig. 5. One-dimensional chains, columns and tubes listed in Table 3. Two-connected vertices are represented by dots whose size shows view depth. The fractional height of nodes for helical units is obtained by dividing the displayed numbers by R (Table 4).

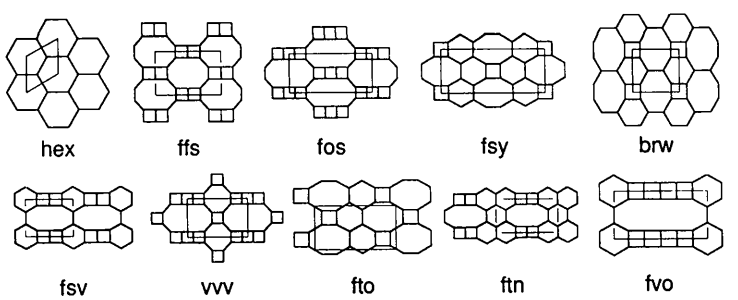

Fig. 6. Two-dimensional three-connected nets listed in Table 3. Crystallographic (one-sided) 2D unit cells are represented by thin lines.

Table 5. *Fractional atomic coordinates* ($x/y/z \times 1000$: *top, four-connected; bottom, two-connected*) *for the most feasible nets in their topologically highest symmetry; unit-cell parameters are given in Table* 2

Net 389	Net 391	Net 392	Net 394	Net 398	Net 400	Net 551	Net 725	Net 959
440/911/154	337/241/363	000/318/584	082/978/169	251/105/167	207/000/000	164/969/825	420/078/642	946/748/236
120/589/154	663/219/341	276/227/861	106/249/312	001/222/167	000/136/117	165/693/649	409/437/629	053/000/245
149/897/328	626/509/327	664/195/916	417/978/168	126/437/162	000/774/160			
851/602/199	340/507/178	956/163/195	410/251/188		250/885/250			
309/751/110	500/200/390	787/201/719	249/955/135	102/139/181	292/948/117	000/018/806	405/257/633	017/625/349
322/920/267	320/359/244	204/350/712	061/105/269	078/328/229	123/074/084	217/000/000	533/020/532	014/750/000
632/975/240	256/111/300	009/218/408	020/851/268	963/235/000	000/222/012	264/051/704	508/508/000	997/874/355
500/000/000	265/286/516	000/500/500	000/000/000	288/093/000	000/172/279	174/806/789	502/241/369	750/737/250
179/521/235	674/365/266	173/205/075	246/293/211	179/422/000	128/824/213	000/667/603	500/500/250	000/000/000
000/500/000	712/104/228	193/042/787	143/250/500	000/500/156		250/750/500		250/007/250
979/079/240	589/500/500	530/307/872	485/854/266	250/000/250				
945/749/265	489/563/238	835/266/078	500/000/000	364/188/241				
147/896/513	345/500/000	500/000/000	435/106/267	250/500/250				
			447/250/000					

Smith (1986). In the highest space group for alternation, the R_{DLS} factor is 0.0079. DLS refinement in the experimental space group of $AlPO_4$-15 [$P2_1/b11$ (14)] results in an R_{DLS} factor of 0.0065 with the assumption of T-atom alternation and 0.0027 with one overall T–O distance. This might indicate that the fully (4;2)-connected net 400 is geometrically feasible, with the assumption of a space group symmetry considerably lower than the topologically highest symmetry.

Net 551 is the most feasible new net. It is built up by an alternation of two types of 2D layers that share a common 'fee' net: the first, (i), consists of 'kew' chains sharing six-rings; the second, (ii), is made up of 'thr' chains sharing opposite crankshaft chains ('*c*'). Together with the (4;2)-connected analogue of $AlPO_4$-12 (Parise, 1984*a*) (catalogue no. 398), net 551 belongs to a polytypic series of structures built up by any sequence of (i) and (ii). The pure end members of this series are ABW (built from (i) only] and the (4;2)-connected net related to the metavariscite structure [built from (ii) only]. Net 398 is related to net 551 by application of the same displacement vector to adjacent 'fee' nets, in contrast to the opposite displacement directions visualized in Fig. 1(*b*). In terms of the 2D layer structures mentioned above, net 398 has the sequence (i)–(i)–(ii). Polytypic materials are common among zeolites. When a stacking fault repeats in a regular pattern, a new material is obtained. For example, polytypism is very common in the ABC-6 group of zeolites and stacking disorder might also interrelate the structures of beryllonite and kaliophilite. The net 551 topology can otherwise be described as a space-filling arrangement of 'kza' 1D units. Descriptions of $AlPO_4$-12 and related net 398 are given by Bennett, Dytrych, Pluth, Richardson & Smith (1986). In the highest space group for alternation, the R_{DLS} factor for net 551 is 0.0013. It is unclear why the simple net 551, as well as net 398 (highest space group for alternation $R_{DLS} = 0.0025$), have not been observed so far.

Net 725 is the (4;2)-connected net underlying the $AlPO_4$-CJ2 structure (Yu, Pang & Li, 1990). Lowering the space group symmetry to that for alternation reduces the R_{DLS} factor to 0.0029. Direct-methods analysis of powder X-ray diffraction data (Kirchner, 1993) indicates that zeolite Linde J (Breck & Acara, 1961) may be isotypic with net 725, consistent with ^{29}Si and ^{27}Al nuclear-magnetic-resonance spectroscopic data and the tetragonal symmetry (powder X-ray diffraction, consistent with $P4_12_12$) observed for NH_4^+ exchanged Linde J samples (Andries, 1989, unpublished). Structure refinement is in progress.

Net 959 is built from 1D ladder-like units (made up of fused four-rings sharing opposite edges and found also in nets 392, 393 and 394) that are connected in a flexible way. Lowering the space group symmetry to that for alternation does not reduce the R_{DLS} factor considerably.

DLS-refined atomic coordinates for nets 389, 391, 392, 394, 398, 400, 551, 725 and 959 are given in Table 5. The top part of this table lists the tetrahedral vertices, the bottom part gives two-connected (O) atom positions.

Nets 400 and 725 are the two highest-symmetry nets obtained here and are geometrically feasible. Both, however, are built from the lowest-symmetry 2D pattern in Table 1. As long as 3D space group determination is not computerized, this finding does not encourage the search for feasible high-symmetry 3D nets using enumeration studies such as the one presented here. Nets 400 and 725 are not really ahead of the other feasible nets, with the exception of net 551, considering their R_{DLS} factors in the topologically highest space group. In contrast, however, to the other feasible nets (389, 391, 392 and 394 with a rather low topological symmetry), both nets relax considerably with lowering of the space group symmetry.

DLS refinements were applied to the observed mixed-coordinated structures of $AlPO_4$-15 (Pluth, Smith, Bennett & Cohen, 1984) and $AlPO_4$-CJ2 (Yu,

Pang & Li, 1990). In $AlPO_4$-CJ2, aluminium is in trigonal bipyramidal (five two-conected oxygen neighbours, hereinafter denoted O[2]) or in octahedral (five O[2] and one F[1] ligand) coordination. In $AlPO_4$-15, two types of octahedral aluminium are found: the first is coordinated with four O[2] and two OH[3]; the second has four O[2], one OH[3] and one H_2O[1] ligands. In both structures, Al–O–Al bridges occur. We used averages of experimentally observed first- and second-neighbour distances where applicable (preserving the overall geometry of the aluminium coordination polyhedra). With weights of 2.0 (P–O), 1.5 (Al–O and Al–F), 1.0 (O–O and O–F) and 0.2 (Al–P and Al–Al), the resulting R_{DLS} factors were 0.0044 ($AlPO_4$–CJ2) and 0.0038 ($AlPO_4$–15). In the latter case, one more distance constraint had to be introduced in order for the one-connected ligand not to move too close to framework O atoms (distance 2.80; weight 0.5). The R_{DLS} factor for $AlPO_4$-CJ2 is higher than for net 725; the one for $AlPO_4$-15 is significantly lower than for net 400 (considering the same space group symmetry with *T*-atom alternation).

Nets 400 and 725 are examples of high-symmetry 3D nets built from low-symmetry 2D patterns with an intersheet linking pattern resulting in non-projecting 2D nets. It is expected that high-symmetry 3D nets built from projecting 2D nets in general result from the connection of high-symmetry 2D patterns. By 'projecting', we mean that adjacent 2D nets have inverted *U*/*D* patterns whereby each node in the 2D net is connected to the same node above or below with an inverted orientation; 2D nets then project in the direction perpendicular to the planar net. Examples of such known framework structures, built from a 2D pattern in Table 1 (number in parentheses) are: ABW (5), GIS (5), paracelsian (1) and the (4;2)-connected analogue of metavariscite (4). Framework structures built from a 2D pattern in Table 1 in combination with a non-projecting intersheet linking pattern different from that in Fig 1(*b*) are: feldspar (6), banalsite (7), YUG (6), MON (2) and the (4;2)-connected relatives of $AlPO_4$-12 (1), variscite (1) and $GaPO_4$-14 (8).

Net 551 and other nets in the same polytypic series (see above) have a rather low topological symmetry (except the pure end members: topological symmetries of ABW and the tetrahedral metavariscite-type net are *Imam* (74) and *I*4/*mmm* (139), respectively) but are geometrically very feasible.

Concluding remarks

Besides net 725, proposed to occur in Linde J, both the tetrahedral analogues of $AlPO_4$-15 and $AlPO_4$-12, as well as net 551, are possible candidates for real materials. It would be interesting to investigate the behaviours of the mixed-coordinated materials upon heating. As observed for $AlPO_4$-53B (Andries, Pluth, Smith, Kirchner & Wilson, 1994) and the calcined form of MCS-1 (Simmen, 1992), both isotypic with the (4;2)-connected analogue of $AlPO_4$-EN3 (Parise, 1985*b*), a transition to a fully (4;2)-connected material might be observed during dehydration (depending on the synthesis conditions).

In relation to net 400, the present results indicate that the mixed-coordinated observed structure is favoured over its (4;2)-connected relative for the same space group symmetry. As mentioned above, comparative theoretical calculations of the structural stabilities of fully (4;2)-connected nets and their observed mixed-coordinated analogues could reveal interesting details.

We thank R. M. Kirchner (Manhattan College, NY) for the direct-methods analysis of Linde J. We acknowledge the Exxon Educational Foundation, UOP, Mobil Research and Development Corporation and Chevron Research & Engineering Corporation for financial aid to the Consortium for Theoretical Frameworks.

References

AKPORIAYE, D. E. (1989). *Z. Kristallogr.* **188**, 103–120.
AKPORIAYE, D. E. (1992). *Zeolites*, **12**, 197–201.
AKPORIAYE, D. E. & PRICE, G. D. (1989). *Zeolites*, **9**, 23–32.
ALBERTI, A. (1979). *Am. Mineral.* **64**, 1188–1198.
ANDRIES, K. J. (1990). *Acta Cryst.* A**46**, 855–868.
ANDRIES, K. J., PLUTH, J. J., SMITH, J. V., KIRCHNER, R. M. & WILSON, S. T. (1994). *Zeolites*. In preparation.
BAERLOCHER, C., HEPP, A. & MEIER, W. M. (1977). *DLS*-76, *a Program for the Simulation of Crystal Structures by Geometric Refinement*. Institut für Kristallographie und Petrographie, ETH, Zürich, Switzerland.
BENNETT, J. M., DYTRYCH, W. J., PLUTH, J. J., RICHARDSON, J. W. & SMITH, J. V. (1986). *Zeolites*, **6**, 349–361.
BRECK, D. W. & ACARA, N. A. (1961). US Patent No. 3 011 869.
BRUNNER, G. O. (1992). *Zeolites*, **12**, 428–430.
DEEM, M. W. & NEWSAM, J. M. (1989). *Nature (London)*, **342**, 260–262.
GOETZKE, K. & KLEIN, H.-J. (1991). *J. Non-Cryst. Solids*, **127**, 215–220.
HAWTHORNE, F. C. & SMITH, J. V. (1988). *Z. Kristallogr.* **183**, 213–231.
International Tables for Crystallography (1983). Vol. A, edited by T. HAHN. Dordrecht: Kluwer Academic Publishers.
KIRCHNER, R. M. (1993). Personal communication.
KOKOTAILO, G. T., FYFE, C. A., GIES, H. & COX, D. E. (1989). *Proceedings of the Eighth International Zeolite Conference, Amsterdam*, edited by P. A. JACOBS & R. A. VAN SANTEN, pp. 715–729. Amsterdam: Elsevier.
KONINGSVELD, H. VAN (1992). *Zeolites*, **12**, 114–120.
KRESGE, C. T., LEONOWICZ, M. E., ROTH, W. J., VARTULI, J. C. & BECK, J. S. (1992). *Nature (London)*, **359**, 710–712.
MARIANS, C. S. & HOBBS, L. W. (1990). *J. Non-Cryst. Solids*, **124**, 242–253.
MEIER, W. M. & OLSON, D. H. (1992). *Atlas of Zeolite Structure Types*, International Zeolite Association Special Publication, 3rd revised ed. London: Butterworths–Heinemann.

O'KEEFFE, M. (1992). *Acta Cryst.* A**48**, 670–673.
PARISE, J. B. (1984*a*). *J. Chem. Soc. Chem. Commun.* pp. 1449–1450.
PARISE, J. B. (1984*b*). *Acta Cryst.* C**40**, 1641–1642.
PARISE, J. B. (1985*a*). *J. Chem. Soc. Chem. Commun.* pp. 606–607.
PARISE, J. B. (1985*b*). *Zeolites*, edited by B. DRZAJ, S. HOCEVAR & S. PEJOVNIK. *Stud. Surf. Sci. Catal.* **24**, 271–278. Amsterdam: Elsevier.
PLUTH, J. J., SMITH, J. V., BENNETT, J. M. & COHEN, J. P. (1984). *Acta Cryst.* C**40**, 2008–2011.
SIMMEN, A. (1992). PhD thesis No. 9710, Institut für Kristallographie und Petrographie, ETH, Zürich, Switzerland.
SMITH, J. V. (1977). *Am. Mineral.* **62**, 703–709.
SMITH, J. V. (1978). *Am. Mineral.* **63**, 960–969.
SMITH, J. V. (1988). *Chem. Rev.* **88**, 149–182.
SMITH, J. V. & BENNETT, J. M. (1984). *Am. Mineral.* **69**, 104–111.
SMITH, J. V. & DYTRYCH, W. J. (1986). *Z. Kristallogr.* **175**, 31–36.
SMITH, J. V. & RINALDI, F. (1962). *Mineral. Mag.* **33**, 202–212.
STIXRUDE, L. & BUKOWINSKI, M. S. T. (1990). *Am. Mineral.* **75**, 1159–1169.
TREACY, M. M. J., RAO, S. & RIVIN, I. (1992). Paper presented at the Ninth International Zeolite Conference, Montreal, Canada, 5–10 July 1992.
WELLS, A. F. (1977). *Three-Dimensional Nets and Polyhedra.* New York: Wiley-Interscience.
WOOD, I. G. & PRICE, G. D. (1992). *Zeolites*, **12**, 320–327.
YU, L., PANG, W. & LI, L. (1990). *J. Solid State Chem.* **87**, 241–244.

Acta Cryst. (1994). A**50**, 325–329

Strengthening of Quartet Invariant Estimates *via* the Prior Estimation of Triplet Relationships

BY M. C. BURLA

Dipartimento di Scienze della Terra, Universitá, 06100 Perugia, Italy

AND G. CASCARANO, C. GIACOVAZZO AND A. GUAGLIARDI

Instituto di Ricerca per lo Sviluppo di Metodologie Cristallografiche CNR, c/o Dipartimento Geomineralogico, Campus Universitario, 70124 Bari, Italy

(*Received* 18 *June* 1993; *accepted* 14 *October* 1993)

Abstract

Formulas for estimating quartet invariants depend on prior information on triplet invariants. If this coincides with the Cochran estimate then the classical quartet formulas [Hauptman (1975). *Acta Cryst.* A**31**, 680–687; Giacovazzo (1976). *Acta Cryst.* A**32**, 91–99, 100–104] are obtained. A mathematical theory is described that improves quartet estimates by exploiting some prior information on triplets. Special emphasis is devoted to the prior estimate of triplet invariants provided by the P_{10} formula.

Symbols

N = number of atoms in the primitive unit cell. For unequal-atom structures, N is replaced in the formulas by $N_{eq} \simeq \sigma_2^3/\sigma_3^2$, where $\sigma_i = \sum_{j=1}^{N} z_j^i$. z_j is the atomic number of the jth atom.
$E_{\mathbf{h}} = R_{\mathbf{h}} \exp(i\varphi_{\mathbf{h}})$, normalized structure factor of index $\mathbf{h}$.
$\varepsilon_i = R_i^2 - 1$
$\Phi = \varphi_{\mathbf{h}} + \varphi_{\mathbf{k}} + \varphi_{\mathbf{l}} + \varphi_{\mathbf{m}}$, with $\mathbf{h} + \mathbf{k} + \mathbf{l} + \mathbf{m} = 0$.
$E_1 = E_{\mathbf{h}}$, $E_2 = E_{\mathbf{k}}$, $E_3 = E_{\mathbf{l}}$, $E_4 = E_{\mathbf{m}}$, $E_5 = E_{\mathbf{h}+\mathbf{k}}$, $E_6 = E_{\mathbf{h}+\mathbf{l}}$, $E_7 = E_{\mathbf{k}+\mathbf{l}}$
$G_{ijp} = 2R_iR_jR_p/N^{1/2}$
$G_{ijpq} = 2R_iR_jR_pR_q/N$
$D_1(x) = I_1(x)/I_0(x)$ = ratio of modified Bessel functions of orders one and zero, respectively.

Introduction

In some recent papers (Giacovazzo, Burla & Cascarano, 1992; Burla, Cascarano & Giacovazzo, 1992; Altomare, Burla, Cascarano, Giacovazzo & Guagliardi, 1993) new attention has been devoted to the practical role of the quartet invariants in direct phasing procedures. A practical recipe was provided: the combined active use of positive estimated quartets and of triplets is not advised. The first reason for this is the well known correlation between positive quartets and positive triplets. The second is the lower accuracy of quartet estimates, which is very remarkable when triplets are estimated *via* the P_{10} formula (Cascarano, Giacovazzo, Camalli, Spagna, Burla, Nunzi & Polidori, 1984). Since P_{10} estimates triplets *via* their second representation (Giacovazzo, 1977), *i.e. via* the special quintets

$$\psi_5 = \varphi_{\mathbf{h}} + \varphi_{\mathbf{k}} - \varphi_{\mathbf{h}+\mathbf{k}} + \varphi_{\mathbf{n}} - \varphi_{\mathbf{n}}, \qquad (1)$$

©1994 International Union of Crystallography
Printed in Great Britain – all rights reserved